

Distribution of hydrogen and helium in the upper atmosphere*

G. KOCKARTS

Institut d'Aéronomie Spatiale de Belgique, 3 Avenue Circulaire,
B-1180, Bruxelles, Belgium

(Received 25 April 1972)

Abstract—A general review of the principal parameters influencing the helium and hydrogen distributions is presented for several physical conditions which are responsible for the upper atmospheric structure. The main differences between the helium and the hydrogen problems are pointed out. In particular, the effect of vertical transport is not similar for the two components. Helium is mainly dominated by the eddy diffusion coefficient whereas, in the case of hydrogen, the vertical flow is the leading factor. It is also shown how eddy diffusion can play a role in the structure of the helium bulge which is now very well confirmed by satellite observations.

1. INTRODUCTION

A CONSEQUENCE of the high abundance of molecular nitrogen is that the global structure of the Earth's atmosphere below 100 km may be expected to be independent of the height at which diffusive equilibrium begins. Above 100 km, however, the atmospheric structure depends strongly on the nature and on the relative abundance of light constituents such as O, He or H. Assuming diffusive equilibrium above 20 km altitude, CHAPMAN and MILNE (1920) deduced the existence of a helium belt above 150 km. With a high abundance of 10^{-4} for H_2 at ground level, JEANS (1925) concluded, however, that hydrogen should be the major atmospheric component above 75 km. These contradictory conclusions indicate that several major problems had not been solved around 1920. First, it was rather puzzling that no optical emissions of helium and hydrogen could be detected in the auroral features. Second, the diffusion problem was not sufficiently developed to define a good diffusion level.

Aeronomy had to wait until the first rocket observations of the absorption of solar radiation above 100 km were made after the second World War. These observations confirmed the theory developed by NICOLET and MANGE (1954) showing that molecular oxygen was still present at 150 km and that atomic oxygen was not in photoequilibrium with O_2 . The scene was then ready for detailed studies of helium and hydrogen distributions, especially since BATES and NICOLET (1950) showed that atomic hydrogen is created in the mesosphere by molecular dissociation processes in which the photodissociation of water vapour plays a fundamental role.

2. MEASUREMENTS OF HYDROGEN AND HELIUM IN THE UPPER ATMOSPHERE

The first far ultraviolet study of the night sky was made in 1955 by BYRAM *et al.* (1957) and resulted in the discovery of the night Lyman- α glow. BATES and PATTERSON (1961) used this measurement to compute a hydrogen distribution in the thermosphere with a concentration of $8.4 \times 10^6 \text{ cm}^{-3}$ at 100 km altitude. KOCKARTS and NICOLET (1962, 1963) adopted a round figure of 10^7 cm^{-3} at the same height. Since 1960, numerous Lyman- α observations have been made by means of

* Review paper presented at the Conference on theoretical ionospheric models, 14-16 June 1971, The Pennsylvania State University, University Park, Pennsylvania.

rockets and satellites. From an analysis of these observations, DONAHUE (1966) deduced a hydrogen concentration of $3 \times 10^7 \text{ cm}^{-3}$ at 100 km. This value is generally adopted and MEIER and MANGE (1970) have shown that it can be used to explain the OGO 4 observations. Nevertheless, there are also observations, analyzed by MEIER and PRINZ (1970), which seem to indicate hydrogen concentrations between 1.25×10^7 and $2 \times 10^7 \text{ cm}^{-3}$ at 100 km. From a discussion of several Lyman- α and Balmer- α observations, TINSLEY (1969) suggested quite definite seasonal changes in the atomic hydrogen abundance, or large solar cycle changes in the production rate. The Lyman- α observations seem to indicate a variation, or an uncertainty of at least a factor of 2, in the atomic hydrogen concentration at 100 km. It should, however, be realized that the Lyman- α geocoronal observations require the solution of a radiative transfer equation (THOMAS, 1963) in an optically thick atmosphere which is not spherically symmetrical. Temporal variations of thermospheric neutral hydrogen have been deduced from H^+ measurements (BRINTON and MAYR, 1971) using the charge transfer equilibrium relationship between H^+ and atomic oxygen. BRINTON and MAYR (1971) were able to separate the atomic hydrogen variations into three components, namely a solar cycle variation, a 27-day variation and a diurnal variation. The observed day-to-night variation of a factor of 2 is in agreement with the theoretical models of PATTERSON (1966) and MCAFEE (1967) and with the ground-based Balmer- α observations of TINSLEY (1970). Although several techniques are now used for the determination of the atomic hydrogen distribution in the thermosphere and in the exosphere, there are no available measurements in the chemosphere below 100 km.

The importance of helium in the lower exosphere was established by NICOLET (1961) who showed that this constituent is necessary to explain the drag data of the satellite Echo 1 above 1000 km. Since neutral helium can be ionized by solar ultraviolet radiation ($\lambda < 504 \text{ \AA}$), the results of an ion probe experiment (HANSON, 1962) and of retarding potential experiments on Explorer VIII (BOURDEAU and BAUER, 1963) were explained with the help of He^+ ions. After the presence of helium had been well established, the analysis of the drag of several satellites like Explorer 9, 14 and 19 showed that an increase of helium occurs at high latitudes for winter conditions (see KEATING *et al.*, 1970). The concentration over the winter polar thermosphere is approximately three to four times higher than over the summer pole. The winter helium bulge has also been deduced by COOK (1967) from the Echo 2 drag data; moreover, mass spectrometric observations on Explorer 17 (REBER and NICOLET, 1965) indicated a latitudinal variation. The recent mass spectrometric measurements on OGO 6 (REBER *et al.*, 1971) show, however, a larger amplitude for the winter helium bulge. An increase by a factor of approximately 10 has been observed over the winter pole around 500 km altitude. The rocket observations made at White Sands (32°N) give helium concentrations at 120 km between 6×10^6 and $5 \times 10^8 \text{ cm}^{-3}$ (KASPRZAK, 1969), whereas an observation by MÜLLER and HARTMANN (1969) leads to a value of $1.2 \times 10^8 \text{ cm}^{-3}$ at 120 km over Fort Churchill (58°N). It is seen from the previous measurements that the major information on the helium distribution comes from drag data and mass spectrometric observations. There are, however, also optical data which contribute to the knowledge of the helium distribution in the upper atmosphere. The twilight emission

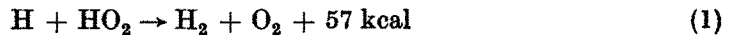
at 10,830 Å, detected since 1958 (see CHRISTENSEN *et al.*, 1971), is attributed to the transition 2^3S-2^3P of orthohelium. Helium is excited in the metastable state by electrons of 20–25 eV and then emits in the infrared. According to CHRISTENSEN *et al.* (1971), these observations are, however, difficult to interpret, since the helium emission at 10,830 Å practically corresponds to emissions of the 5–2 band of the hydroxyl radical OH. The intensity of the emission simultaneously depends on the helium concentration, on the solar flux at $\lambda < 380$ Å giving rise to photoelectrons, and on the conjugate photoelectrons.

The Naval Research Laboratory group (BYRAM *et al.*, 1961) attempted in 1960 to detect the ultraviolet night glow from neutral helium at 584 Å or from ionized helium at 304 Å. The estimated brightness of the glow was less than one tenth of the hydrogen Lyman- α glow. The daytime helium glow at 584 Å has recently been measured by DONAHUE and KUMER (1971) with a retarding potential photometer between 400 and 1000 km. The maximum emission of 0.7 kR was observed at 500 km, whereas the hydrogen Lyman-emission was of the order of 15 kR at the same height. It should finally be mentioned that the recent discovery by JOHNSON *et al.* (1971) of an ionized helium magnetoglow at 304 Å offers a promising technique for dynamical studies of the magnetosphere.

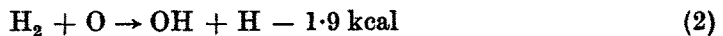
The previously described experimental data are directly related to the physical processes which will be discussed in the following sections.

3. PRODUCTION AND LOSS MECHANISMS

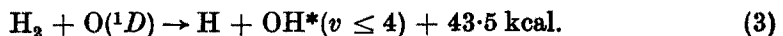
Recently, NICOLET (1970, 1971) discussed in detail the reactions involving atomic hydrogen in the chemosphere. Above the mesopause, the photodissociation of water vapor is the principal production mechanism and the reaction



leads to the production of molecular hydrogen which is destroyed in the thermosphere by



and in the lower mesosphere by



Besides the uncertainties in the rate coefficients, the important production of H_2 at the mesopause and the loss processes of H_2 at the stratopause and in the thermosphere are such that the eddy diffusion transport must play a very important role in the H_2 distribution. Since the values of the eddy diffusion coefficient are not known and since the equilibrium conditions for atomic hydrogen cannot be reached in less than several days, NICOLET (1971) concludes that, at the present time, mixing conditions lead to the best approximation for atomic hydrogen in the lower thermosphere. Therefore, atomic hydrogen concentrations between 10^7 and $3 \times 10^7 \text{ cm}^{-3}$ deduced at 100 km from Lyman experiments (DONAHUE, 1966; MEIER and MANGE, 1970; MEIER and PRINZ, 1970) may reflect in a certain way the variability of the chemospheric processes. Above 100 km atomic hydrogen is subject to molecular diffusion and reaches a critical level where the collision frequency is so low that

Table 1. Escape parameters for hydrogen and helium at 500 km

T ($^{\circ}\text{K}$)	Scale height (km)		Effusion velocity (cm sec^{-1})		H (hr)	Lifetime He (yr)
	H	He	H	He		
750	740	185	9.65×10^1	1.50×10^{-10}	148	2.7×10^9
1000	986	246	8.75×10^2	1.39×10^{-6}	22	3.9×10^5
1250	1233	308	3.24×10^3	3.26×10^{-4}	7.3	2.1×10^3
1500	1479	370	7.71×10^3	1.22×10^{-2}	3.7	6.6×10^1
1750	1726	432	1.42×10^4	1.62×10^{-1}	2.3	5.9×10^0
2000	1973	493	2.25×10^4	1.11×10^0	1.7	9.8×10^{-1}

atoms with enough kinetic energy can escape from the Earth's gravitational field. The escape flow is the product of the concentration by an effusion velocity which can be computed from the velocity distribution function (NICOLET, 1957). Table 1 gives the escape parameters of H and He for several thermopause temperatures. The lifetime is defined as the time necessary to reduce the concentration at 500 km by 50 per cent. It is clear that for temperatures above 1000 $^{\circ}\text{K}$, a time less than one day is sufficient to reduce significantly the atomic hydrogen concentration. Therefore, a diffusion transport from below must compensate the continuous escape flux. Such a flow affects the vertical distribution of hydrogen in the way discussed by BATES and PATTERSON (1961), and by KOCKARTS and NICOLET (1962, 1963).

The physical situation is different for helium-4 which is produced by radioactive decay of uranium and thorium in the crust and in the mantle of the Earth. An important problem is to know what fraction is released in the atmosphere. NICOLET (1957) deduced a generation rate of 1.75×10^6 atoms $\text{cm}^{-2} \text{sec}^{-1}$ and the adopted values are usually of the order of 1×10^6 to 2×10^6 $\text{cm}^{-2} \text{sec}^{-1}$. Recent measurements of the helium-4 profile in the deep sea (CRAIG and CLARKE, 1970) indicate, however, a flux of the order of 7.7×10^5 atoms $\text{cm}^{-2} \text{sec}^{-1}$. Since helium is not transformed by chemical reactions in the homosphere, it follows that there is a mixing distribution with a relative abundance of 5.24×10^{-6} up to the altitude where molecular diffusion becomes effective. In the homosphere, the vertical helium flux is transported by turbulence or by eddy diffusion. In the upper thermosphere it has been shown (KOCKARTS and NICOLET, 1962) that thermal escape can only provide an average dissipation of 6×10^4 $\text{cm}^{-2} \text{sec}^{-1}$ helium atoms over a whole solar cycle. This is due to the small effusion velocities in Table 1 which lead to very long lifetimes. With a flux of 10^6 atoms $\text{cm}^{-2} \text{sec}^{-1}$, the total atmospheric helium content of 1.13×10^{20} cm^{-2} can be obtained in 3.5×10^6 yr. This implies that atmospheric helium has been completely renewed at least 1000 times since the Earth's formation. Therefore, an effective escape mechanism must exist. PATTERSON (1968) reviewed several non-thermal mechanisms which could conceivably resolve the discrepancy between the helium flux released from the Earth's interior and the average thermal escape flux. The most effective mechanism appears to be the loss of helium ions through the polar wind (BANKS and HOLZER, 1968; AXFORD, 1968). Typical values for the polar wind helium flux are approximately $2-4 \times 10^6$ atoms $\text{cm}^{-2} \text{sec}^{-1}$ (BANKS and HOLZER, 1969). The precise global loss rate due to ion escape is difficult to calculate since the boundary between convection and co-rotation of magnetic

field lines is variable. It seems, however, that the combination of thermal escape and polar wind loss is capable of explaining the terrestrial helium balance.

The differences between the production and loss mechanisms of hydrogen and helium will influence the vertical distributions of these constituents in the thermosphere.

4. DIFFUSION TRANSPORT IN THE THERMOSPHERE

A time dependent solution of the thermospheric helium and hydrogen distributions can be obtained from the continuity equation

$$\frac{\partial n_1}{\partial t} + \text{div} (n_1 \mathbf{w}_1) = P - L \quad (4)$$

where \mathbf{w}_1 represents the transport velocity, n_1 the concentration, P and L the production and loss terms respectively. PATTERSON (1970) reviewed extensively the diurnal variation of hydrogen taking into account the lateral flow effect, and concluded that the day-to-night variation is less than a factor 4. In the present section, the vertical component w_1 of the transport velocity will be investigated in relation with the concept of maximum flow (MANGE, 1955, 1961). When the vertical velocity w_1 is considered as being due to molecular and to eddy diffusion, it is possible to show (KOCKARTS, 1971) that

$$w_1 = -D_1 \left[\frac{1}{n_1} \frac{dn_1}{dz} + \frac{1}{H_1} + (1 + \alpha) \frac{1}{T} \frac{dT}{dz} \right] - K \left[\frac{1}{n_1} \frac{dn_1}{dz} + \frac{1}{H} + \frac{1}{T} \frac{dT}{dz} \right] \quad (5)$$

where n_1 is the helium or hydrogen concentration, D_1 and K are respectively the molecular diffusion coefficient and the eddy diffusion coefficient, T is the temperature at height z , H_1 is the pressure scale height of the minor constituent 1, and H is the atmospheric scale height. The thermal diffusion factor α is approximately equal to -0.38 for helium and hydrogen. Introducing the ratio $\Lambda = K/D_1$, the differential equation for the concentration n_1 in a steady state is then

$$\frac{dn_1}{dz} + \left[\frac{1}{1 + \Lambda} \left(\frac{1}{H_1} + \frac{\Lambda}{H} \right) + \left(1 + \frac{\alpha}{1 + \Lambda} \right) \frac{1}{T} \frac{dT}{dz} \right] n_1 = - \frac{F}{D_1(1 + \Lambda)} \quad (6)$$

where the flow $F = n_1 w_1$ is subject to certain continuity conditions which can involve chemical reactions or which are related to the escape process. When the second member of (6) is negligible, the zero flow concentration n_{eq} is given by

$$n_{\text{eq}}(z)/n_1(z_0) = (T_0/T) \exp - \left[\int_{z_0}^z \left(\frac{1}{H_1} + \frac{\Lambda}{H} \right) (1 + \Lambda)^{-1} dz + \int_{z_0}^z \alpha (1 + \Lambda)^{-1} \frac{dT}{T} \right] \quad (7)$$

where z_0 is a reference level.

If $\Lambda = 0$, i.e. there is no turbulence, (7) reduces to the usual diffusive equilibrium solution. If $\Lambda = \infty$, i.e. no molecular diffusion, relation (7) leads to a mixing distribution characterized by a scale height H . The relation (7) actually shows that a smooth transition from perfect mixing to diffusive equilibrium is possible even under zero flow conditions. This can be seen in Fig. 1 which shows several helium distributions computed for different height-independent eddy diffusion coefficients. The helium mixing ratio at 90 km is 5.24×10^{-6} .

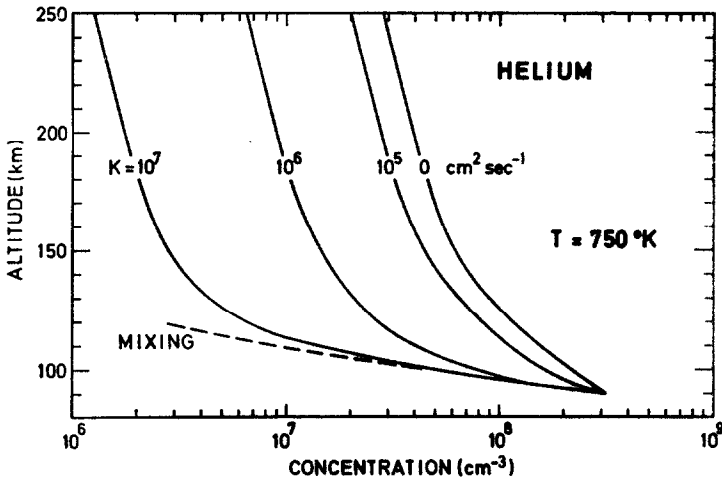


Fig. 1. Helium distribution above 90 km for different values of the eddy diffusion coefficient K in an atmospheric model with a thermopause temperature of 750°K .

When a real flow F is introduced, integration of (6) leads to

$$n_1(z) = n_{\text{eq}} \left[1 - \int_{z_0}^z \frac{F}{D_1(1 + \Lambda)n_{\text{eq}}} dz \right] \quad (8)$$

where n_{eq} is given by (7). Since the integral in (8) is always positive for an upwards flow, it is clear that the presence of such a flow tends to give concentration less than the zero flow solution n_{eq} . Equations (7) and (8) show that any departure from diffusive equilibrium is due either to eddy diffusion or to a transport flow.

The importance of the vertical transport velocity can be analyzed by expressing the concentration scale height of the minor constituent as a function of the total concentration scale height $(1/n)(dn/dz)$ in a form such as

$$\frac{1}{n_1} \frac{dn_1}{dz} = X(z) \frac{1}{n} \frac{dn}{dz} \quad (9)$$

where $X(z)$ is a vertical distribution factor. Using the hydrostatic equation, the transport velocity (5) can be written

$$w_1 = \frac{D_1}{H} \left[X - \frac{H}{H_1} - \frac{H}{T} \frac{dT}{dz} (1 + \alpha - X) \right] + \frac{K}{H} [X - 1]. \quad (10)$$

When the minor constituent follows a mixing distribution, the vertical distribution factor X is equal to unity and the transport velocity arises from molecular diffusion alone. In this case, equation (10) reduces to

$$w_1 = \frac{D_1}{H} \left(1 - \frac{H}{H_1} - \frac{\alpha H}{T} \frac{dT}{dz} \right). \quad (11)$$

When a minor constituent follows a mixing distribution over a certain height range, equation (11) gives the maximum transport velocity arising from molecular diffusion. This velocity is a physical property of the atmosphere which is independent of the

Table 2. Maximum molecular diffusion transport velocity (cm sec⁻¹)

z (km)	H (km)	T (°K)	w_H (cm sec ⁻¹)	w_{He} (cm sec ⁻¹)
85	4.82	160.3	2.29×10^{-1}	1.08×10^{-1}
90	5.34	176.7	6.40×10^{-1}	3.01×10^{-1}
95	5.85	193.0	1.64×10^0	7.63×10^{-1}
100	6.41	209.2	3.78×10^0	1.78×10^0
105	7.24	230.9	8.38×10^0	3.94×10^0
110	8.42	261.9	1.56×10^1	7.35×10^0
115	9.63	293.0	2.82×10^1	1.32×10^1
120	10.87	324.0	4.91×10^1	2.30×10^1

abundance of the minor component. Table 2 shows the maximum molecular diffusion velocities computed for an atmospheric model given by NICOLET (1970, 1971). The molecular diffusion coefficient used in the computations is

$$D_1 = 1.5 \times 10^{18} \left(\frac{1}{M_1} + \frac{1}{M} \right)^{1/2} \frac{T^{1/2}}{n} \text{ (cm}^2 \text{ sec}^{-1}) \quad (12)$$

where M_1 and M are respectively the minor constituent mass and the atmospheric mean molecular mass expressed in atomic mass units. The numerical factor in (12) depends of course on the adopted momentum transfer cross section. It is seen from Table 2 that the maximum diffusion velocity around 100 km is of the order of a few cm sec⁻¹. These molecular diffusion velocities are of the same order of magnitude as the vertical motions deduced by JOHNSON and GOTTLIEB (1970) from the global asymmetry in the solar heating at the solstice. However, the diffusion velocity is always upwards for hydrogen and helium, since their atomic masses are smaller than the atmospheric mean molecular mass.

The importance of a flow on the vertical distribution can be estimated by comparing the maximum flow to the real flow. For atomic hydrogen, a concentration of $3 \times 10^7 \text{ cm}^{-3}$ at 100 km leads to a maximum flow $F_M(H) \simeq 10^8 \text{ cm}^{-2} \text{ sec}^{-1}$ which is comparable to the real flow originating from the mesosphere. The hydrogen distributions show on Fig. 2 indicate that the flow is responsible for the steep slope of the curves in the neighbourhood of 100 km. The flow effect is more pronounced than the effect of eddy diffusion. For helium, a concentration of $5 \times 10^7 \text{ cm}^{-3}$ at 100 km leads to a maximum flow $F_M(He) \simeq 9 \times 10^7 \text{ cm}^{-2} \text{ sec}^{-1}$. The real flow of the order of $10^6 \text{ cm}^{-2} \text{ sec}^{-1}$ is, however, negligible compared to the maximum flow, and the second member in equation (6) has practically no effect on the helium distribution. Figure 1 is therefore computed using equation (7).

Since the molecular diffusion coefficient increases exponentially with height, the second member in (6) becomes numerically less important at great altitude, even in the case of atomic hydrogen. Therefore, the vertical distribution has a tendency to become similar to a diffusive equilibrium distribution in the upper thermosphere. Since the diffusion equation is no longer valid in the exosphere, an upward diffusion flux must be controlled by an escape mechanism at the base of the exosphere. Thermal escape is the most effective mechanism for atomic hydrogen (see Table 1). But a controversy arose several years ago about the validity of the effusion velocity computed using a Maxwellian velocity distribution function. It

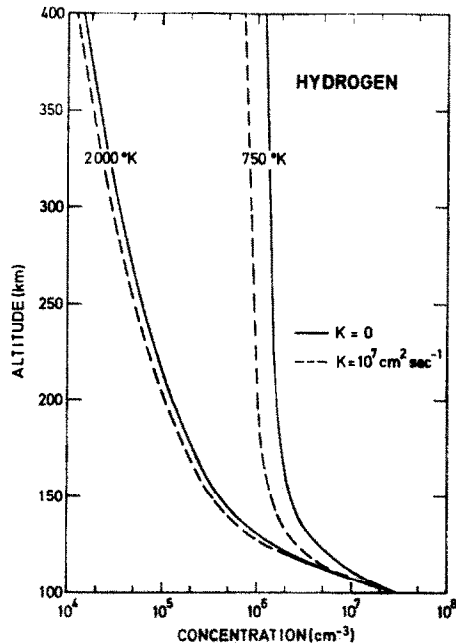


Fig. 2. Hydrogen distribution for two atmospheric models with thermopause temperatures of 750°K and 2000°K respectively.

appears now (CHAMBERLAIN and SMITH, 1971; BRINKMANN, 1971) that the effusion velocity of Jeans, given in Table 1, should not be reduced by more than 25 per cent in the case of atomic hydrogen. Since it is difficult to claim an absolute accuracy better than 25 per cent for the hydrogen concentration, the introduction of this type of correction will not basically modify the vertical distribution of hydrogen in the thermosphere. For helium, the problem is less important, since thermal evaporation is not the predominant escape mechanism.

5. EFFECT OF EDDY DIFFUSION

It is clear from the discussion of the general solution (8) that two extreme cases can occur in the upper atmosphere.

(1) The real flow of the particles is negligible compared to the maximum diffusion flow: this is the case for helium.

(2) The real flow of the particles is of the same order of magnitude as the maximum diffusion flow: this is the case for atomic hydrogen.

An intermediate case is illustrated by the behaviour of deuterium (KOCKARTS, 1972).

When the real flow is negligible in the diffusion equation, the adopted value for the eddy diffusion coefficient K strongly influences the vertical distribution. The results shown in Fig. 1 have been obtained with constant values of K . It is nevertheless established (see JOHNSON and GOTTLIEB, 1970; KENESHEA and ZIMMERMAN, 1970) that turbulent diffusion is a function of altitude. Thus, it is necessary to analyse the effect of a height-dependent eddy diffusion coefficient. Since there are practically no experimental determinations of K above 90 km, more or less arbitrary values have to be used. From an analysis of the rates of heat input and heat losses

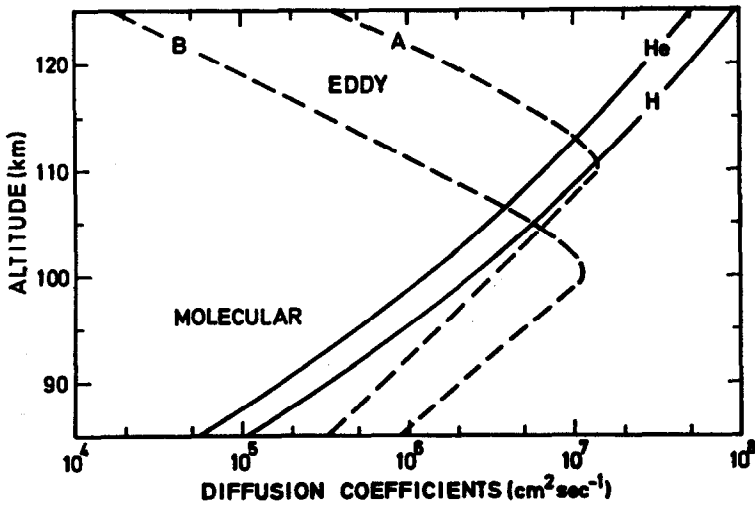


Fig. 3. Molecular and eddy diffusion coefficients as a function of altitude. The distributions A and B are respectively used for the computation of the concentrations labelled A and B in Fig. 4.

in the mesosphere and in the lower thermosphere, JOHNSON and GOTTLIEB (1970) deduced a worldwide average eddy diffusion coefficient. The curve A shown in Fig. 3 is consistent with the results obtained by JOHNSON and GOTTLIEB (1970), whereas curve B cannot be excluded *a priori*. The molecular diffusion coefficients of helium and hydrogen, computed from equation (12), are represented by the full curves. The height at which $K = D_1$ is sometimes called the turbopause. With such a definition, the turbopause height is not the same for all the atmospheric components. Figure 4 shows the helium distribution obtained with the eddy diffusion coefficients of curves A and B in Fig. 3. The helium distributions for variable K fall between the curves corresponding respectively to the constant values $K = 10^6 \text{ cm}^2 \text{ sec}^{-1}$ and $K = 10^7 \text{ cm}^2 \text{ sec}^{-1}$. Both constant and variable eddy diffusion coefficients lead to a smooth transition from perfect mixing to diffusive equilibrium.

Mass spectrometric observations analyzed by KASPRZAK (1969) sometimes indicate helium concentration gradients larger than the usual diffusive equilibrium gradients. Figures 1 and 4 clearly show that such slopes can be obtained by the introduction of turbulent diffusion. It is therefore not necessary to introduce vertical fluxes which eventually cannot be transported by diffusion. The effect of eddy diffusion can also be presented in the form shown on Fig. 5. For a height independent K value between 10^5 and $10^7 \text{ cm}^2 \text{ sec}^{-1}$, the helium concentration at 120 km altitude can vary by more than a factor of 10. The observations analyzed by KASPRZAK (1969) give, at 120 km, helium concentrations ranging from $5 \times 10^8 \text{ cm}^{-3}$ to $6 \times 10^6 \text{ cm}^{-3}$. The highest value would imply that diffusive equilibrium starts well below 90 km, whereas the flux of $2.6 \times 10^{10} \text{ atoms cm}^{-2} \text{ sec}^{-1}$ introduced by KASPRZAK (1969) is well above the maximum diffusion flow. Because of the great sensitivity of the helium distribution to the K values, it is difficult to perform a detailed analysis of a particular observation when simultaneous information on the vertical distribution of K is not available. The altitude at which the eddy diffusion

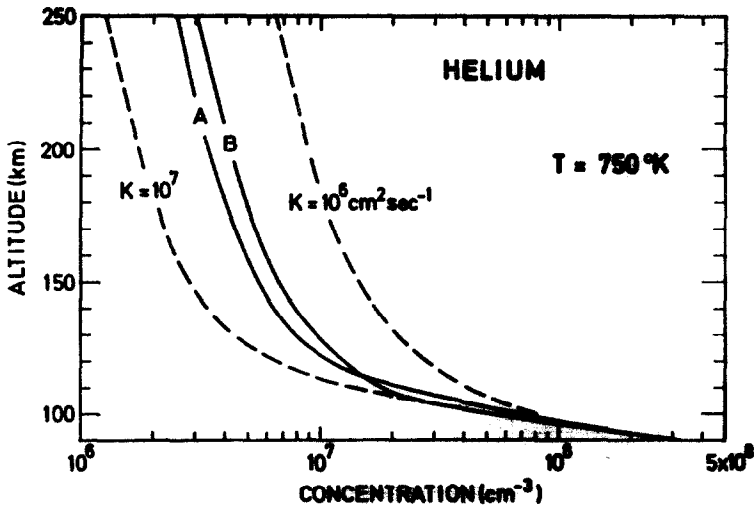


Fig. 4. Helium distributions for the height dependent eddy diffusion coefficient given in Fig. 3. The dashed curves corresponding to constant K values are shown for comparison.

coefficient passes through a maximum between the mesopause and 120 km is, for instance, an important parameter. Since the available information on the variations of K in the lower thermosphere is still too scarce, height-independent values are used to indicate an order of magnitude of the resulting phenomena. It should, however, be kept in mind that the eddy diffusion coefficient sharply decreases above the height where $K = D_1$ (KENESHEA and ZIMMERMAN, 1970).

Turbulent diffusion produces less effect (see Fig. 2) on the atomic hydrogen distribution, since the transport flux around 100 km is such that hydrogen practically follows a mixing distribution even for $K = 0$. Some difficulties can, however, arise for thermopause temperatures below 1000°K. At 120 km altitude, Fig. 6 shows that

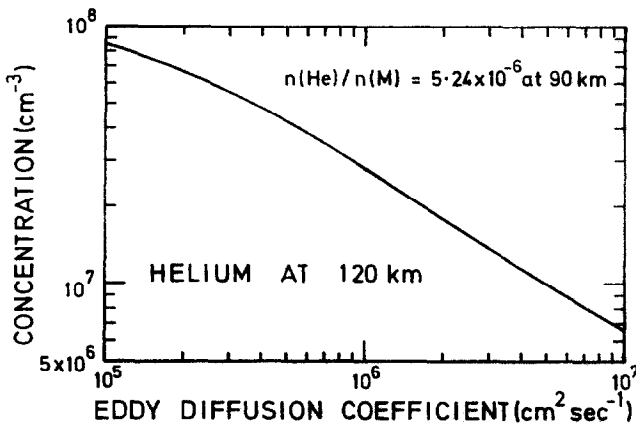


Fig. 5. Helium concentration at 120 km as a function of height-independent eddy diffusion coefficients.

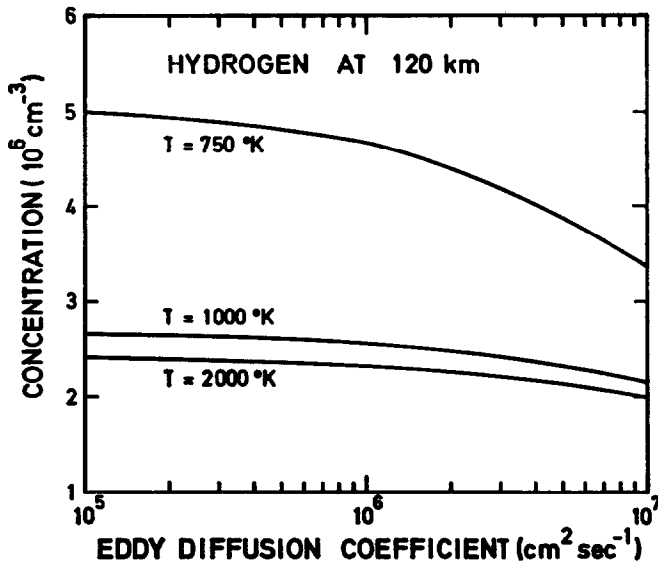


Fig. 6. Atomic hydrogen concentration at 120 km as a function of height-independent eddy diffusion coefficients for thermopause temperatures of 750°K, 1000°K and 2000°K.

atomic hydrogen decreases by a factor of 2 for a thermopause temperature of 750°K when K increases from $10^5 \text{ cm}^2 \text{ sec}^{-1}$ to $10^7 \text{ cm}^2 \text{ sec}^{-1}$. For temperatures above 1000°K, the effect of eddy diffusion is practically negligible. This situation is directly related to the thermal escape flux given in Table 3 for an altitude of 1000 km. It is seen that the thermal escape flux decreases when the temperature falls below 1000°K (KOCKARTS and NICOLET, 1962). The influence of eddy diffusion then becomes more pronounced. When the total atomic hydrogen content (Fig. 7) is plotted as a function of the thermopause temperature, the effect of eddy diffusion is again predominant below 1000°K. Therefore the interpretation of Lyman- α observations is more difficult during solar minimum conditions, since an increase of the optical depth can be due either to a decrease of the eddy diffusion coefficient or to an increase of the boundary concentration around 100 km altitude.

Another difficulty results from the ionic polar wind (BANKS and HOLZER, 1969; LEMAIRE and SCHERER, 1970) which can be more important than the maximum diffusion flux for temperatures below 1000°K. Because of this, the thermospheric hydrogen distribution could be thoroughly altered in the polar region during minimum solar activity. The effect of the polar wind on the thermospheric helium distribution is, however, less important, since the ion flux ($\approx 2 \times 10^6 \text{ cm}^{-2} \text{ sec}^{-1}$) is

Table 3. Atomic hydrogen thermal escape flux ($\text{cm}^{-2} \text{ sec}^{-1}$) at 1000 km

K ($\text{cm}^2 \text{ sec}^{-1}$)	Temperature (°K)					
	600	700	800	900	1000	2000
0	4.3×10^7	8.4×10^7	9.9×10^7	1.0×10^8	1.0×10^8	1.0×10^8
10^6	3.5×10^7	7.5×10^7	9.3×10^7	9.9×10^7	1.0×10^8	1.0×10^8
10^7	1.4×10^7	4.3×10^7	6.7×10^7	7.9×10^7	8.3×10^7	8.4×10^7

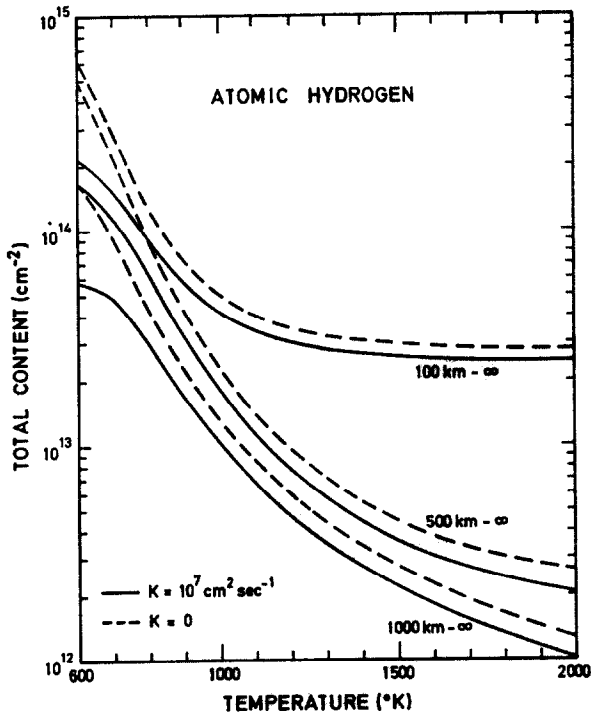


Fig. 7. Vertical total content of atomic hydrogen above 100 km, 500 km and 1000 km as a function of the thermopause temperature. The adopted concentration at 100 km is $3 \times 10^7 \text{ cm}^{-3}$.

still negligible compared to the maximum diffusion flux. The helium polar wind is principally involved in the global budget without any fundamental perturbation of the thermospheric distribution.

6. THE WINTER HELIUM BULGE

Several explanations have been proposed for the winter helium bulge. KOCKARTS and NICOLET (1962, 1963) have shown that a decrease of 5 km in the helium diffusion level leads to an increase by a factor of 2 in the helium concentration in the thermosphere. Several authors (COOK, 1967; KEATING and PRIOR, 1968) used this fact as a possible explanation for the variation, by a factor of 4, between the winter and summer polar regions. Recently JOHNSON and GOTTLIEB (1970) estimated a horizontal inflow towards the winter polar region associated with a vertical upward flow above the turbopause. Such a wind system could provide an explanation for the above mentioned increase, by a factor of 4, towards the winter polar region. Figure 5 shows nevertheless that a latitudinal variation, by a factor of 10, in the eddy diffusion coefficient could also lead to an increase by a factor of 4 in the helium concentration. The recent mass spectrometric observations by REBER *et al.* (1971) show, however, that the helium density over the winter polar region is greater than in summer by a factor of 10. Thus either the wind system of JOHNSON and GOTTLIEB (1970) should be more intense, or the latitudinal variation in the eddy diffusion

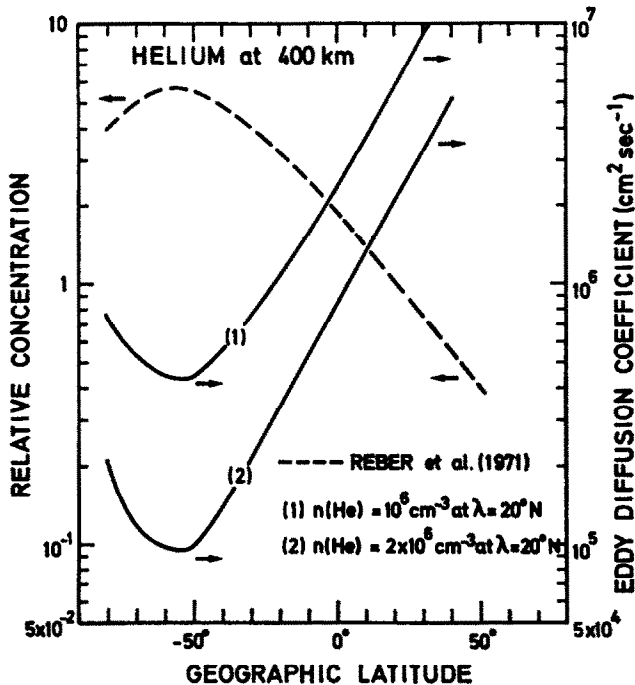


Fig. 8. Latitudinal variation of the eddy diffusion coefficient required for an explanation of the mass spectrometric observations made on OGO 6 in June 1969.

coefficient should be more pronounced. In Fig. 8, an example of the measurements by REBER *et al.* (1971) is represented by the dashed line as a function of geographic latitude. When these data are normalized to an absolute concentration $n(\text{He}) = 10^6 \text{ cm}^{-3}$ at a latitude of 20°N , the eddy diffusion coefficients given by curve (1) are required to explain the observations with a 1000°K atmospheric model. The model temperature is not a crucial parameter since, at 400 km, the helium concentration is not strongly dependent on the thermopause temperature for a fixed value of K . When the data are normalized to $2 \times 10^6 \text{ cm}^{-3}$ at 20°N , the eddy diffusion coefficients are given by curve (2). It is seen in both cases that the eddy diffusion coefficient should decrease by approximately a factor of 50 between the summer and winter hemispheres. The question is to determine whether such latitudinal variations of K are possible or not. According to the theory presented by JOHNSON and GOTTLIEB (1970), it is clear that the eddy diffusion coefficient is much smaller over the polar winter region, since less energy has to be conducted downwards by turbulent transport. The observed decrease in the helium concentration around $\lambda = -60^\circ\text{S}$ (REBER *et al.*, 1971) could then be due to a particular heating process in the winter polar region, such as Joule heating (COLE, 1971; BANKS, 1972). The increase in the heat input requires larger eddy diffusion coefficients around 100 km for the downwards heat conduction.

If the helium bulge is due to a latitudinal variation of K , an atomic oxygen bulge should also appear. The amplitude of the latitudinal atomic oxygen variation should, however, be much smaller. First of all, the effect of eddy diffusion is more

important for light constituents. Secondly, in the winter polar region the photo-dissociation coefficient of O_2 is drastically reduced and less atomic oxygen is produced. A final answer is, however, not possible without time-dependent computations of the atomic oxygen distribution including latitudinal variations. Although wind and temperature data indicate (ZIMMERMAN *et al.*, 1972) that the winter polar mesosphere is more turbulent than the summer polar mesosphere, not enough data are available between 90 km and 120 km to investigate a latitudinal variation of K in this region.

7. SUMMARY

In the case of atomic hydrogen, the major difficulties preventing a complete understanding of the thermospheric distribution come from the lack of knowledge of the transport mechanisms in the lower thermosphere. Although there is some uncertainty concerning the rate coefficients of the numerous reactions in which the hydrogen compounds are involved, a more precise determination of the eddy diffusion coefficient is required in the whole homosphere. When the boundary concentration around 100 km is determined, it is then possible to compute vertical distributions which are practically independent of the adopted eddy diffusion coefficient. Below 1000°K serious problems can, however, occur in the polar regions since the ion polar wind can produce a depletion of the thermospheric hydrogen.

In the case of helium, the vertical flux is not the major factor influencing the distribution, since it is always negligible compared to maximum diffusion flow. It has been shown that precise values are required for the eddy diffusion coefficient, since this parameter is able to produce important variations in the vertical distribution. It is, however, not excluded that a wind system (JOHNSON and GOTTLIEB 1970) can produce a contribution to the observed latitudinal variation. Nevertheless, the possibility of a latitudinal dependence of the eddy diffusion cannot be excluded at the present time.

Acknowledgements—The author wishes to express his gratitude to Dr. C. REBER for providing him with some unpublished data of the helium mass spectrometric measurements made on OGO 6.

REFERENCES

- | | | |
|--|------|---|
| AXFORD W. I. | 1968 | <i>J. geophys. Res.</i> 73 , 6855. |
| BANKS P. M. | 1972 | <i>Space Research XII</i> . North-Holland, Amsterdam. |
| BANKS P. M. and HOLZER T. E. | 1968 | <i>J. geophys. Res.</i> 73 , 6846. |
| BANKS P. M. and HOLZER T. E. | 1969 | <i>J. geophys. Res.</i> 74 , 6317. |
| BATES D. R. and NICOLET M. | 1950 | <i>J. geophys. Res.</i> 55 , 301. |
| BATES D. R. and PATTERSON T. N. L. | 1961 | <i>Planet. Space Sci.</i> 5 , 257. |
| BOURDEAU R. E. and BAUER S. J. | 1963 | <i>Space Research III</i> , p. 173. North-Holland, Amsterdam. |
| BRINKMANN R. T. | 1971 | <i>Planet. Space Sci.</i> 19 , 791. |
| BRINTON H. C. and MAYR H. G. | 1971 | <i>J. geophys. Res.</i> 76 , 6198. |
| BYRAM E. T., CHUBB T. A. and FRIEDMAN H. | 1961 | <i>J. geophys. Res.</i> 66 , 2095. |
| BYRAM E. T., CHUBB T. A., FRIEDMAN H. and KUPPERIAN J. | 1957 | <i>The Threshold of Space</i> (Edited by M., ZELIKOFF), p. 203. Pergamon Press, London. |
| CHAMBERLAIN J. W. and SMITH G. R. | 1971 | <i>Planet. Space Sci.</i> 19 , 675. |

- CHAPMAN S. and MILNE E. A. 1920 *Q. J. R. met. Soc.* **46**, 357.
- CHRISTENSEN A. B., PATTERSON T. N. L. 1971 *J. geophys. Res.* **76**, 1764.
and TINSLEY B. A.
- COLE K. D. 1971 *Planet. Space Sci.* **19**, 59.
- COOK G. E. 1967 *Planet. Space Sci.* **15**, 627.
- CRAIG H. and CLARKE W. B. 1970 *Earth planet. Sci. Letts* **9**, 45.
- DONAHUE T. M. 1966 *Annls Géophys.* **22**, 175.
- DONAHUE T. M. and KUMER J. B. 1971 *J. geophys. Res.* **76**, 145.
- HANSON W. B. 1962 *J. geophys. Res.* **67**, 183.
- JEANS J. H. 1925 *The Dynamical Theory of Gases*, p. 340.
Dover, New York.
- JOHNSON F. S. and GOTTLIEB B. 1970 *Planet. Space Sci.* **18**, 1707.
- JOHNSON C. Y., YOUNG J. M. and 1971 *Science* **171**, 379.
HOLMES J. C.
- KASPRZAK W. T. 1969 *J. geophys. Res.* **74**, 894.
- KEATING G. M. and PRIOR E. J. 1968 *Space Research VIII*, p. 982. North-
Holland, Amsterdam.
- KEATING G. M., MULLINS J. A. and 1970 *Space Research X*, p. 439. North-Holland
Prior E. J. Amsterdam.
- KENESHEA T. J. and ZIMMERMAN S. P. 1970 *J. atmos. Sci.* **27**, 831.
- KOCKARTS G. 1971 *Physics of the Upper Atmosphere* (Edited
by F. VERNIANI), p. 330. Casa Editrice
Compositori, Italy.
- KOCKARTS G. 1972 *Space Research XII*. North-Holland,
Amsterdam.
- KOCKARTS G. and NICOLET M. 1962 *Annls Géophys.* **18**, 269.
- KOCKARTS G. and NICOLET M. 1963 *Annls Géophys.* **19**, 370.
- LEMAIRE J. and SCHERER M. 1970 *Planet. Space Sci.* **18**, 103.
- MANGE P. 1955 *Annls Géophys.* **11**, 153.
- MANGE P. 1961 *Annls Géophys.* **17**, 277.
- McAFEE J. R. 1967 *Planet. Space Sci.* **15**, 599.
- MEIER R. R. and MANGE P. 1970 *Planet. Space Sci.* **18**, 803.
- MEIER R. R. and PRINZ D. K. 1970 *J. geophys. Res.* **75**, 6969.
- MULLER D. and HARTMANN G. 1969 *J. geophys. Res.* **74**, 1287.
- NICOLET M. 1957 *Annls Géophys.* **13**, 1.
- NICOLET M. 1961 *J. geophys. Res.* **66**, 2263.
- NICOLET M. 1970 *Annls Géophys.* **26**, 531.
- NICOLET M. 1971 *Mesospheric Models and Related Experi-*
ments (Edited by G. FIOCCO), p. 1.
Reidel, Dordrecht.
- NICOLET M. and MANGE P. 1954 *J. geophys. Res.* **59**, 15.
- PATTERSON T. N. L. 1966 *Planet. Space Sci.* **14**, 425.
- PATTERSON T. N. L. 1968 *Rev. Geophys.* **6**, 553.
- REBER C. A. and NICOLET M. 1965 *Planet. Space Sci.* **13**, 617.
- REBER C. A., HARPOLD D. N., 1971 *J. geophys. Res.* **76**, 1845.
HOROWITZ R. and HEDIN A. E.
- THOMAS G. E. 1963 *J. geophys. Res.* **68**, 2639.
- TINSLEY B. A. 1969 *Atmospheric Emissions* (Edited by B. M.
McCORMAC and A. OMHOLT), p. 539.
Van Nostrand Reinhold.
- TINSLEY B. A. 1970 *Space Research X*, p. 582. North-
Holland, Amsterdam.
- ZIMMERMAN S. P., FAIRE A. C. and 1972 *Space Research XII*. North-Holland,
Murphy E. A. Amsterdam.